Solar Wind Plasma Interaction with Gerasimovich Lunar Magnetic Anomaly

Shahab Fatemi[1,2], Andrew R. Poppe[1,2], Gregory T. Delory[1,2], Charles Lue[3], Mats Holmstrom[3]

1. Space Sciences Laboratory, UC Berkeley, CA, USA
2. SSERVI, NASA Ames Research Center, CA, USA
3. Swedish Institute of Space Physics, Kiruna, Sweden

July 23, 2015

Why is it interesting?

- The Moon has small-scale crustal magnetic fields

- Solar wind plasma interaction with lunar crustal fields

- Correlation between crustal magnetic fields and lunar swirls

Why is it interesting?

- The Moon has small-scale crustal magnetic fields

- Solar wind plasma interaction with lunar crustal fields

- Correlation between crustal magnetic fields and lunar swirls

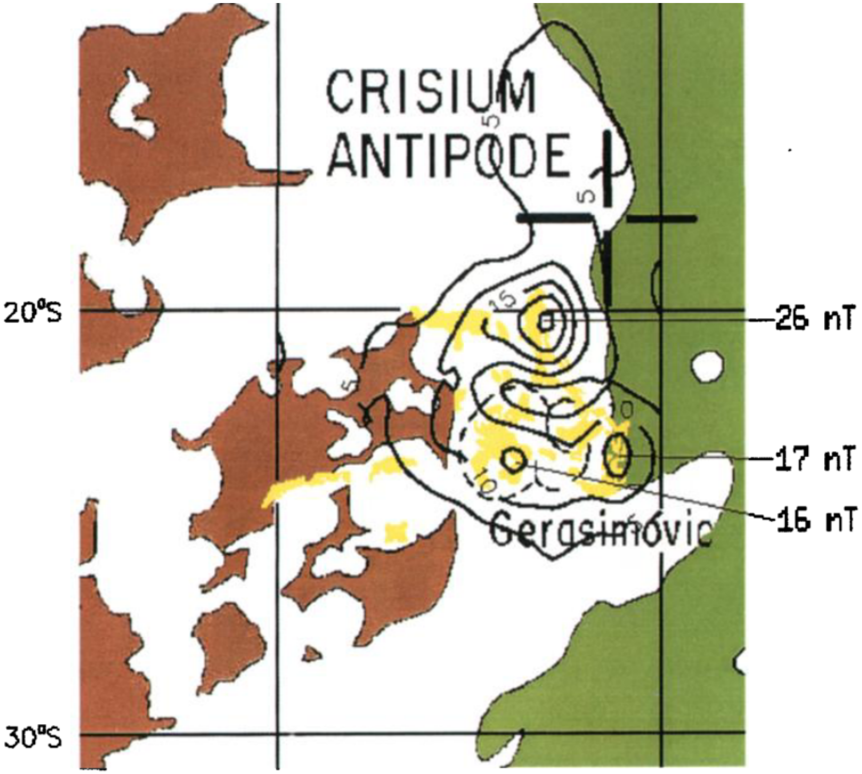

[Hood et al., 2001]

Global image of interaction

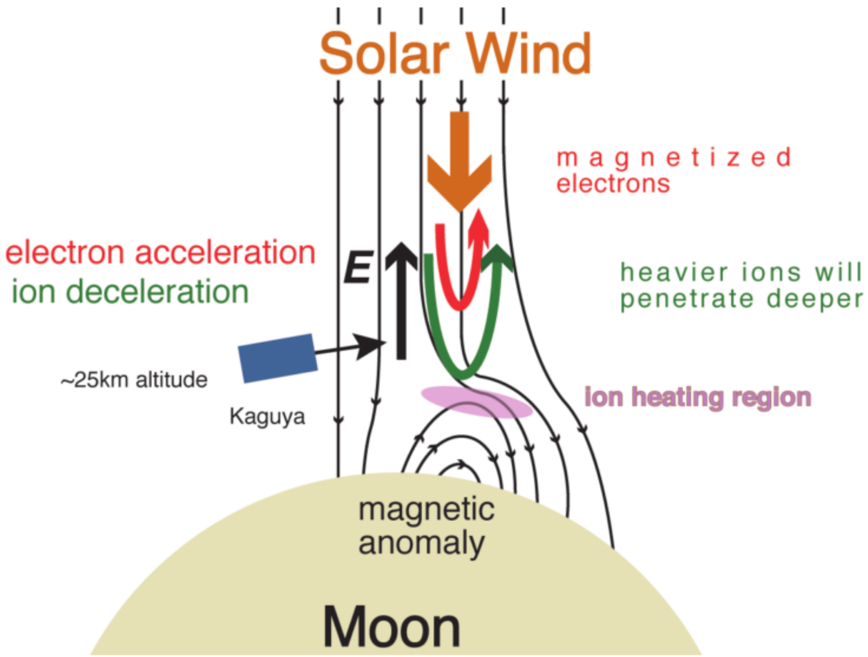

[Saito et al., 2012]

- Magnetized electrons reflect at high altitudes

- Heavy ions penetrate deeper

- Ambipolar electric field

Global image of interaction

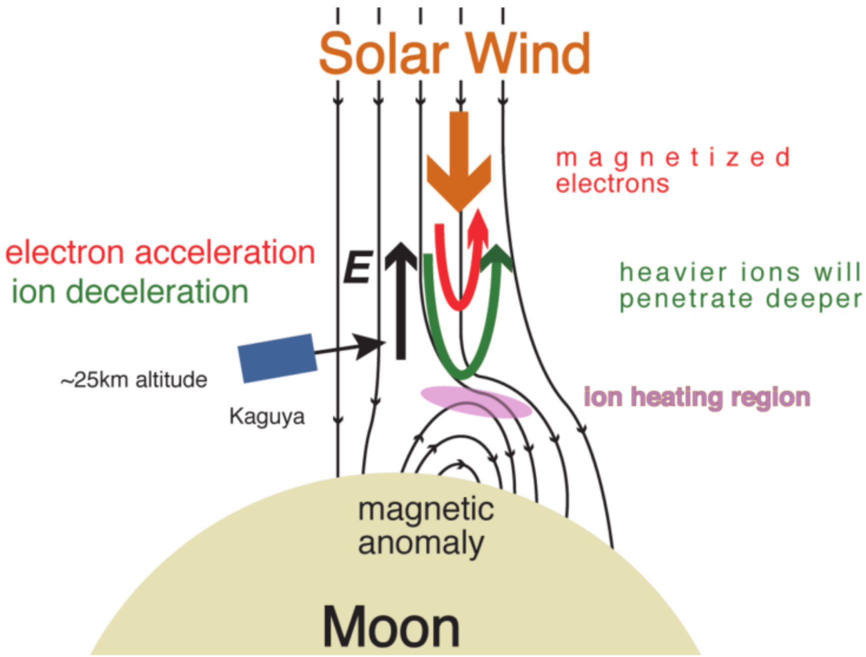

[Saito et al., 2012]

Chandrayaan-1 estimation of electrostatic potential through ENA observation.

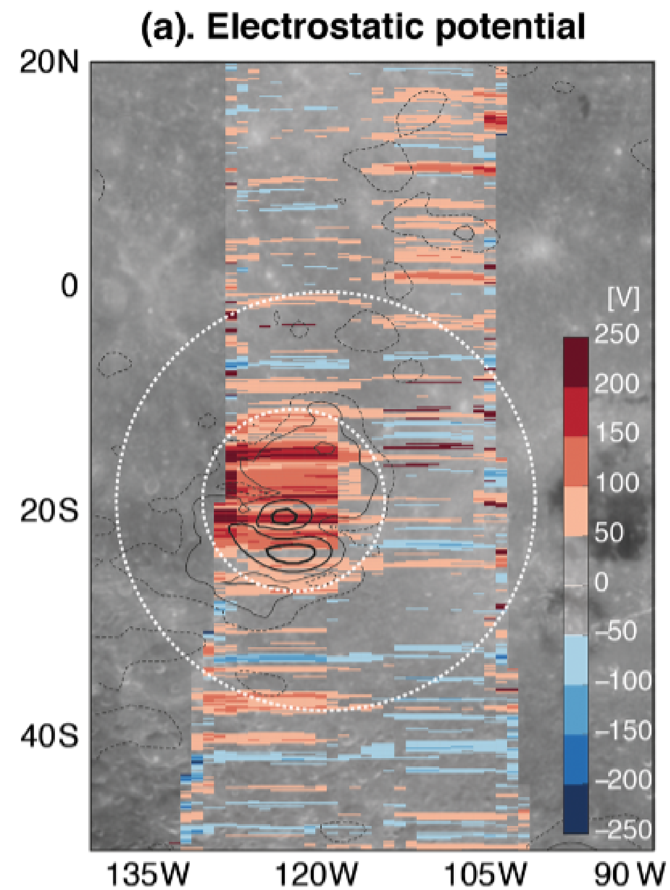

[Futaana et al., 2013]

- Magnetized electrons reflect at high altitudes
- Heavy ions penetrate deeper
- Ambipolar electric field

Modeling plasma interaction with anomalies

- Previous theoretical and numerical works:
    * MHD, Particle-in-cell (PIC), and Hybrid

- Here we use:
    * Three-dimensional self-consistent hybrid model of plasma (ions are kinetic particles, electrons are a massless fluid) [Holmstrom, 2010, 2013].

    * include an empirical model of lunar crustal magnetization Developed by Purucker and Nicholas, 2010.

Modeling plasma interaction with anomalies

- Previous theoretical and numerical works:
    * MHD, Particle-in-cell (PIC), and Hybrid

- Here we use:
    * Three-dimensional self-consistent hybrid model of plasma
      (ions are kinetic particles, electrons are a massless fluid)
      [Holmstrom, 2010, 2013].

    * include an empirical model of lunar crustal magnetization
      Developed by Purucker and Nicholas, 2010.

30 km altitude

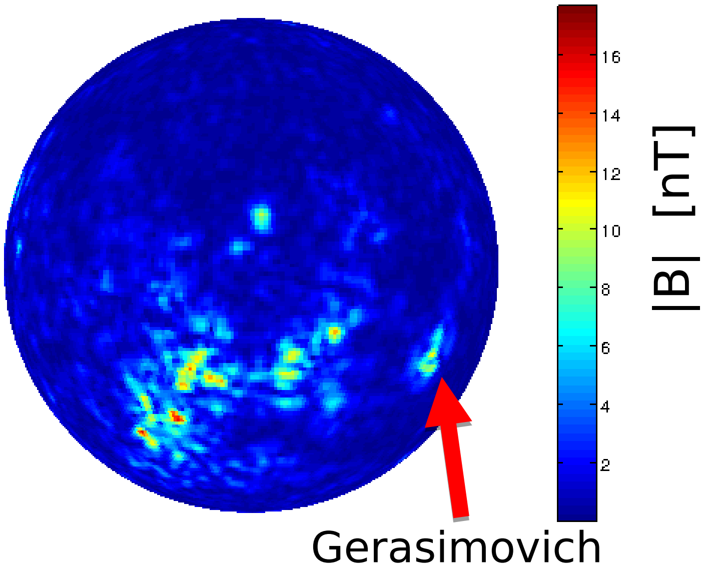

20 km altitude

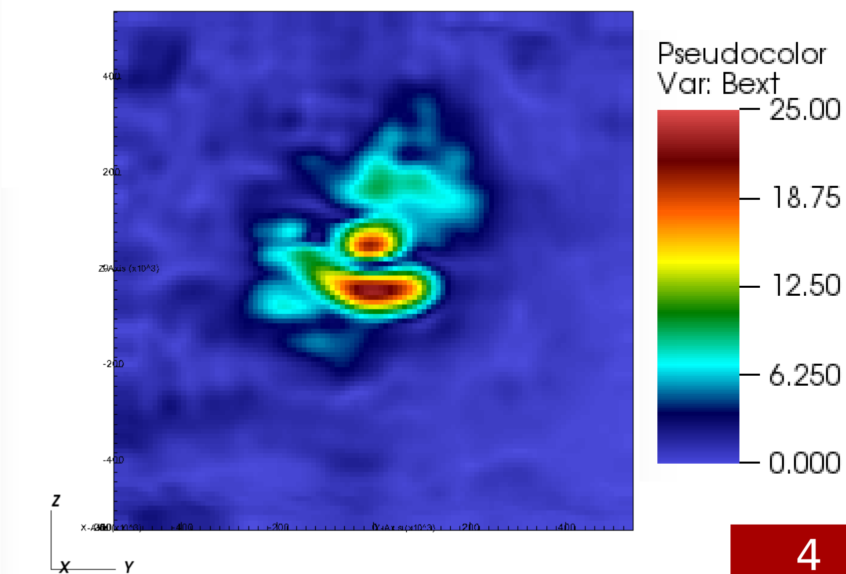

Coordinate system & parameters

- Solar wind flows along the surface normal vector (x-axis)
- Solar wind speed is 310 km/s
- Interplanetary magnetic field (IMF) magnitude is 4 nT.
- Proton temperature is ~4 eV, and electron temperature is ~10 eV.

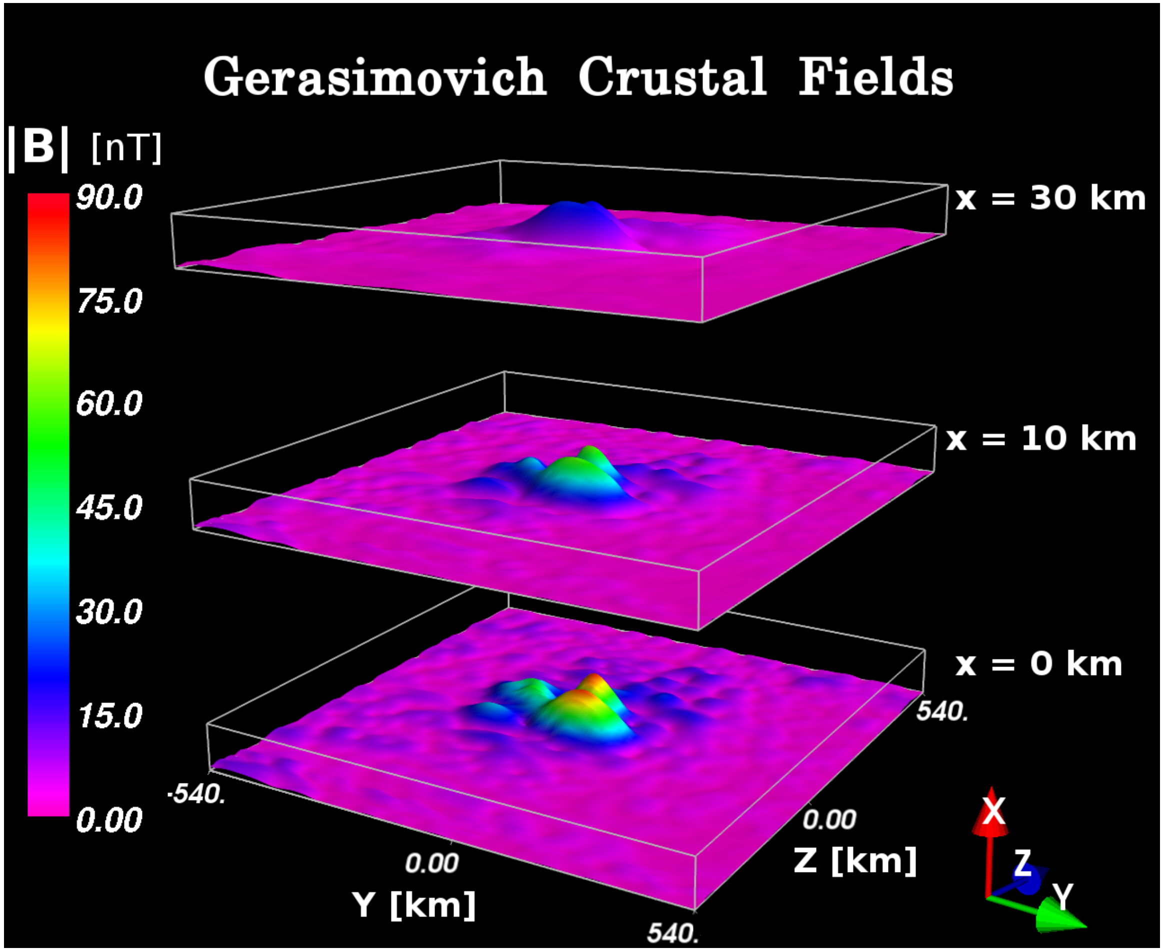

Run	n_i [cm^{-3}]	P_{dyn} [nPa]
Low	3.5	0.6
Medium	**7.0**	**1.2**
High	14.0	2.4

Model results (medium P_{dyn})

- Crustal fields are compressed and disturbed by the solar wind

- Downgoing protons are decelerated and deflected around crustal fields.

- Surface is locally shielded

- Protons are reflected over the crustal field

- Average reflection flux is ~10% of the incident flux

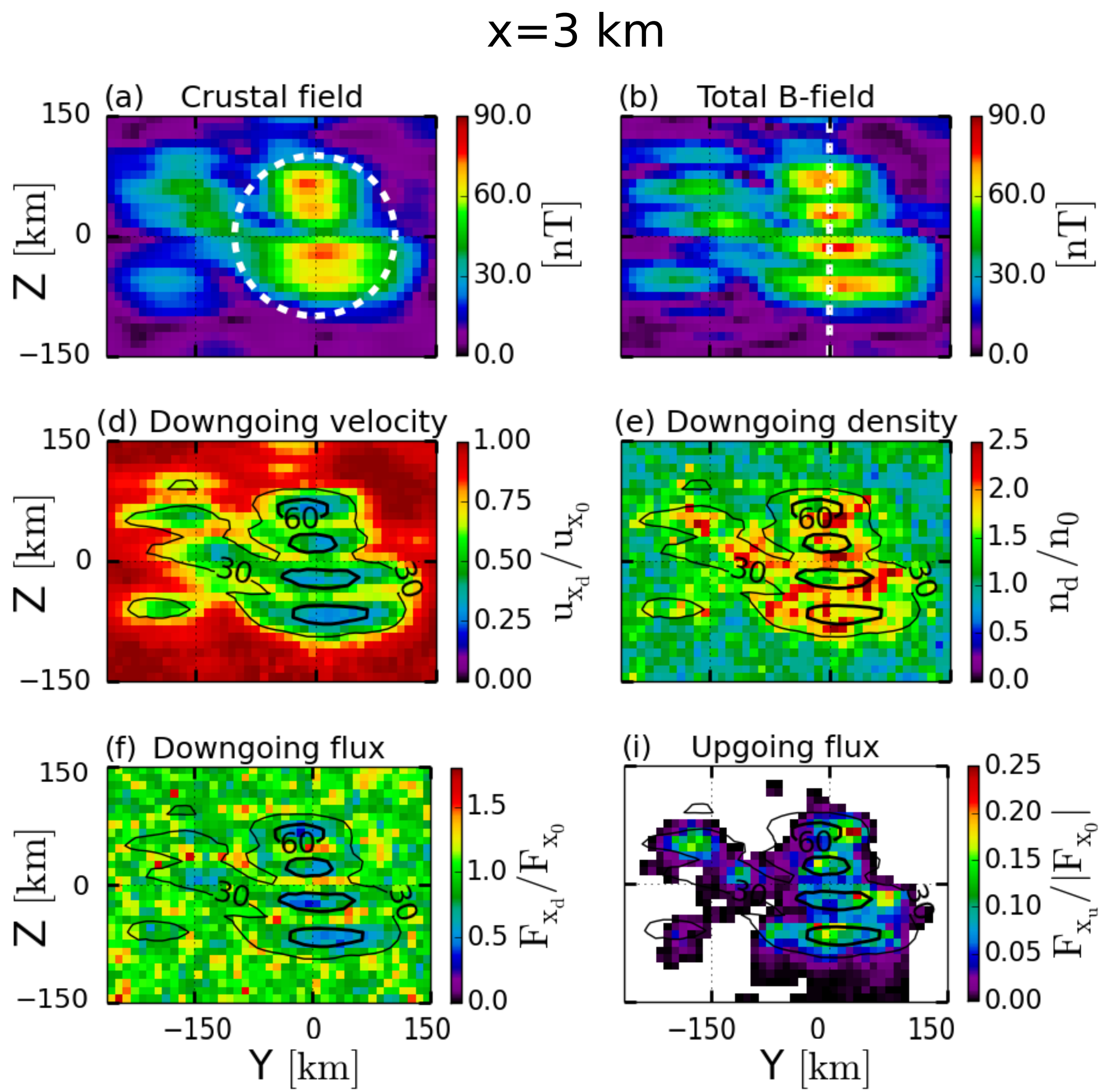

[Fatemi et al., 2015]

Effects of plasma dynamic pressure

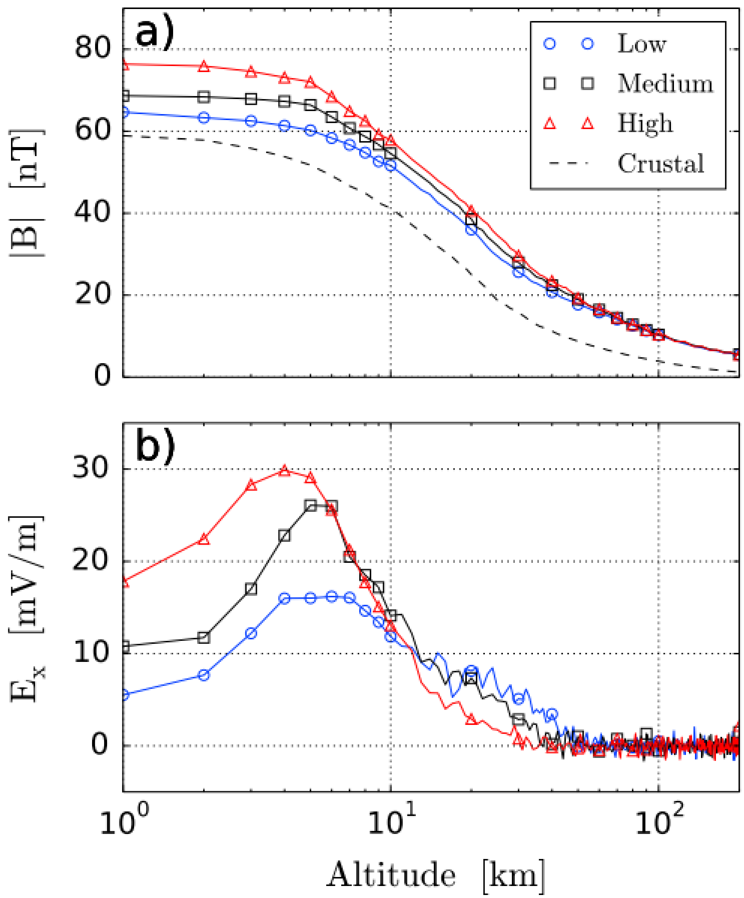

[Fatemi et al., 2015]

- Crustal fields are compressed by the solar wind.

- Magnetic fields get stronger close to the surface when the dynamic pressure increases.

- Solar wind ions start to decelerate at higher altitudes during low dynamic pressures.

- Electric field closer to the surface (<10 km) is stronger for high dynamic pressures.

- On average, a potential of nearly+300 V forms at the surface under the Gerasimovich crustal fields, which is consistent with observations.

Different components of electric field

Electric field in our hybrid model

$$\mathbf{E} = \frac{1}{\rho_i}\left(-\mathbf{J}_i \times \mathbf{B} + \mu_0^{-1}\left(\nabla \times \mathbf{B}\right) \times \mathbf{B} - \nabla p_e\right)$$

Different components of electric field

Electric field in our hybrid model

$$\mathbf{E} = \frac{1}{\rho_i}\left(\underbrace{\boxed{-\mathbf{J}_i \times \mathbf{B}}}_{\text{Convective}} + \underbrace{\boxed{\mu_0^{-1}\left(\nabla \times \mathbf{B}\right) \times \mathbf{B}}}_{\text{Hall term}} - \underbrace{\boxed{\nabla p_e}}_{\text{Ambipolar}}\right)$$

Different components of electric field

Electric field in our hybrid model

$$\mathbf{E} = \frac{1}{\rho_i}\left(\boxed{-\mathbf{J}_i \times \mathbf{B}} + \boxed{\mu_0^{-1}(\nabla \times \mathbf{B}) \times \mathbf{B}} - \boxed{\nabla p_e}\right)$$

Convective   Hall term   Ambipolar

- Previous works suggested that the Hall term is the dominant electric field over the lunar crustal field (e.g. Saito et al., 2012; Jarvinen et al., 2014).

- Ambipolar electric field has a noticeable contribution at close distances to the Moon.

Anti-moon ward electric fields

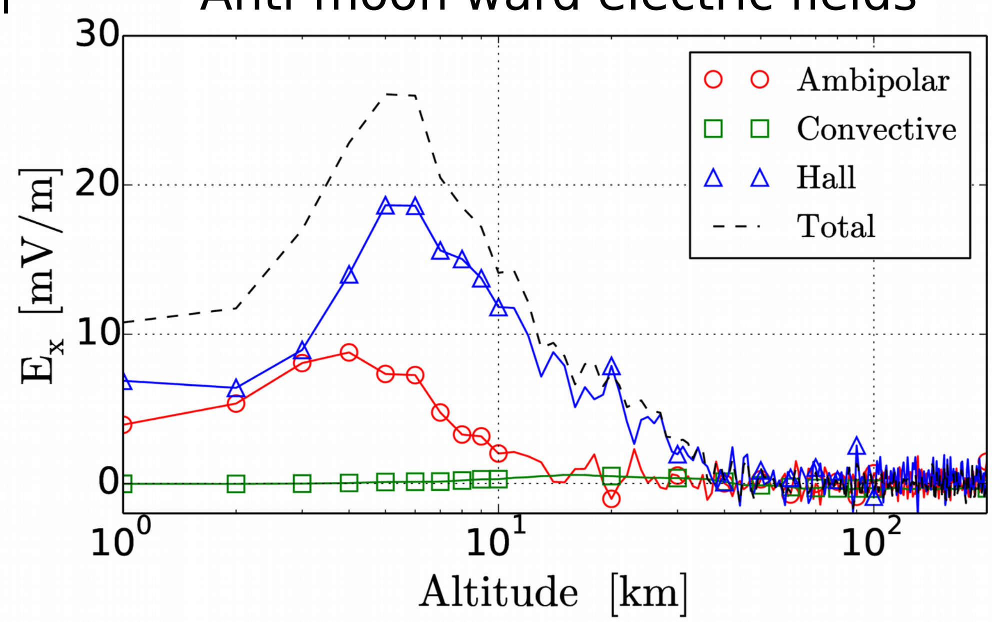

[Fatemi et al., 2015]

Summary!

- The first local hybrid simulations for the solar wind interaction with realistic lunar crustal field.

- The incident solar wind flux to the lunar surface is considerably reduced over the crustal fields.

- The effects of low and high solar wind dynamic pressures.

- Low P_{dyn} => deflects plasma
  High P_{dyn} => reflects plasma

- Anti-moonward Hall electric field is the dominant electric field, but the ambipolar electric field has a noticeable contribution to the electric field at close distances (<3 km) to the Moon.

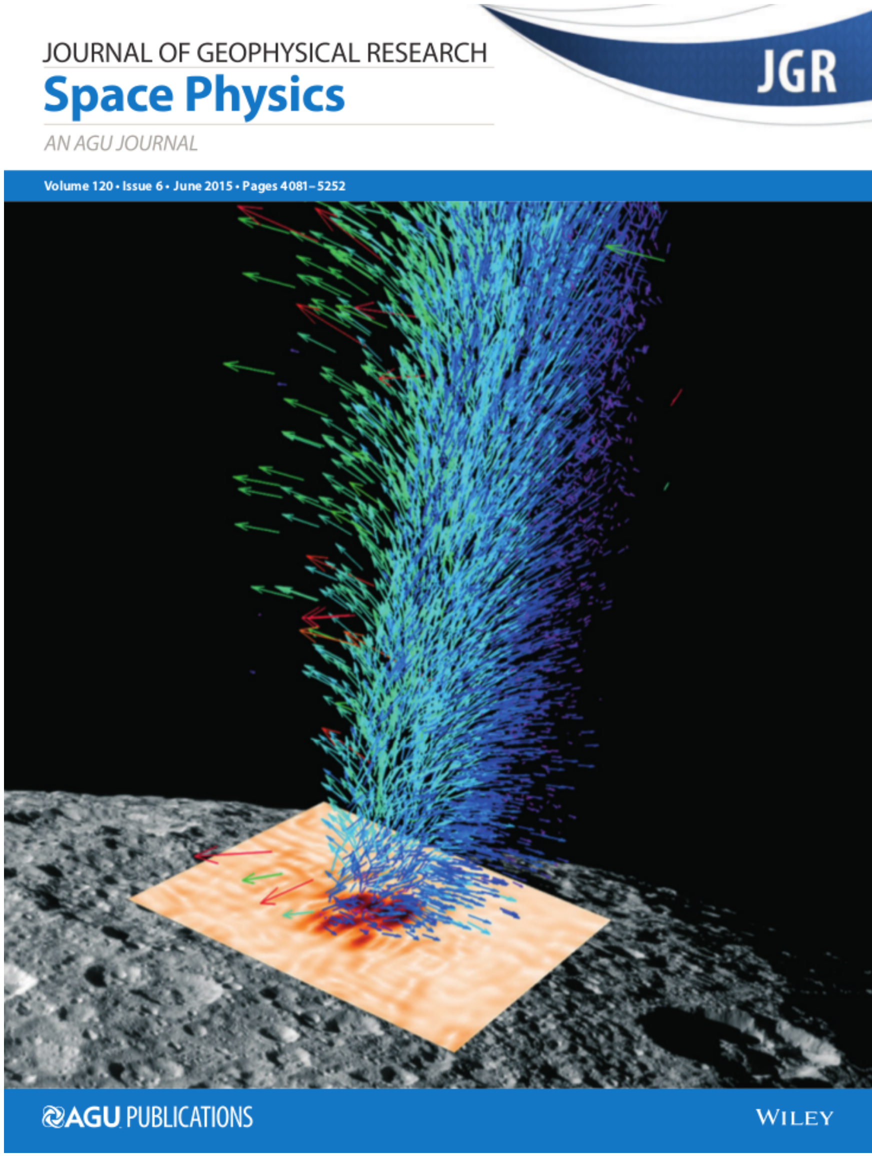

Backup

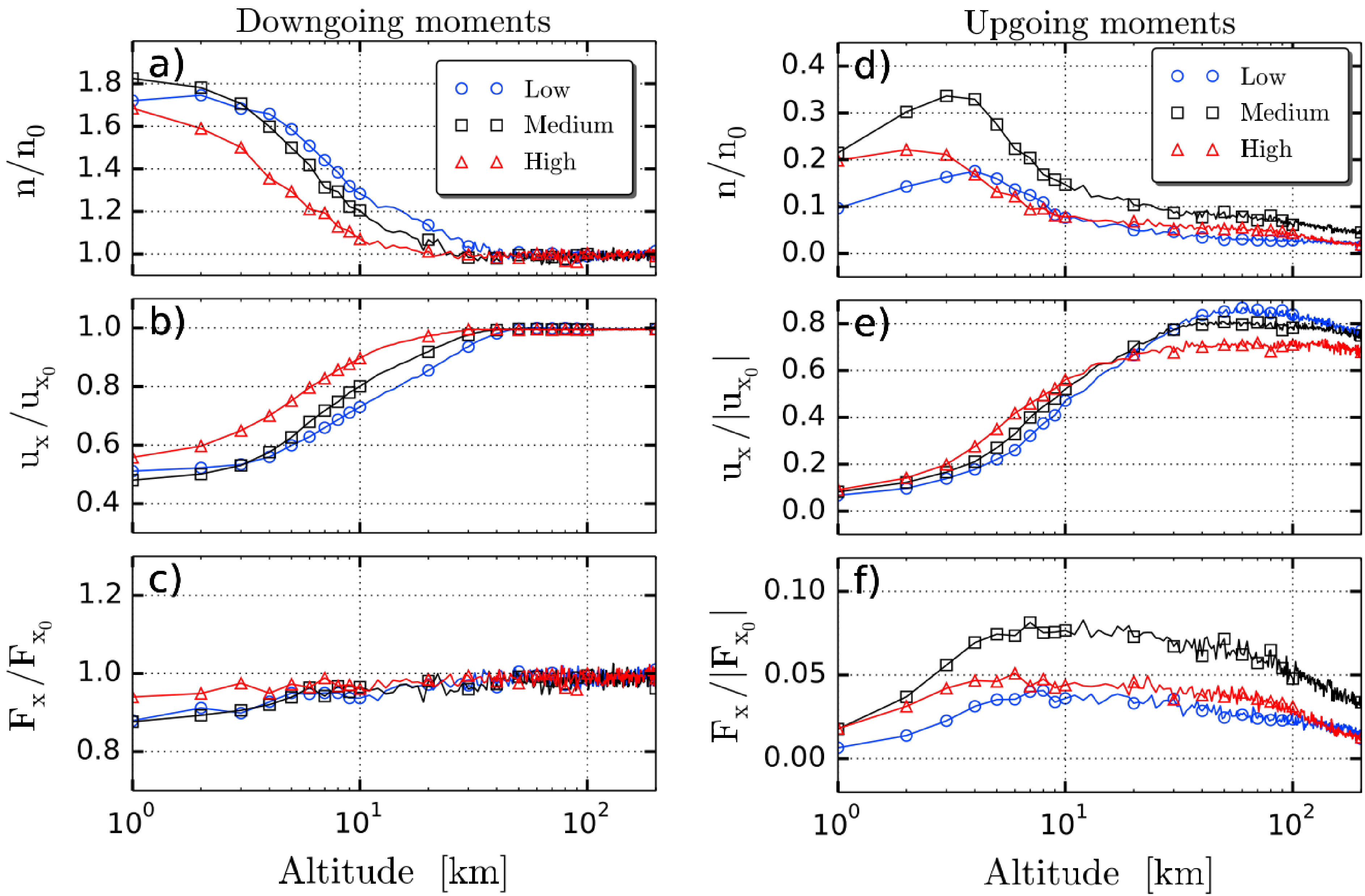

Downgoing moments
Upgoing moments
a)
b)
c)
d)
e)
f)
Low
Medium
High
n/n0
ux /ux0
Fx /Fx0
ux /|ux0|
Fx /|Fx0|
1.8
1.6
1.4
1.2
1.0
0.8
0.6
0.4
0.3
0.2
0.1
0.0
0.10
0.05
0.00
10^0
10^1
10^2
Altitude [km]

Backup

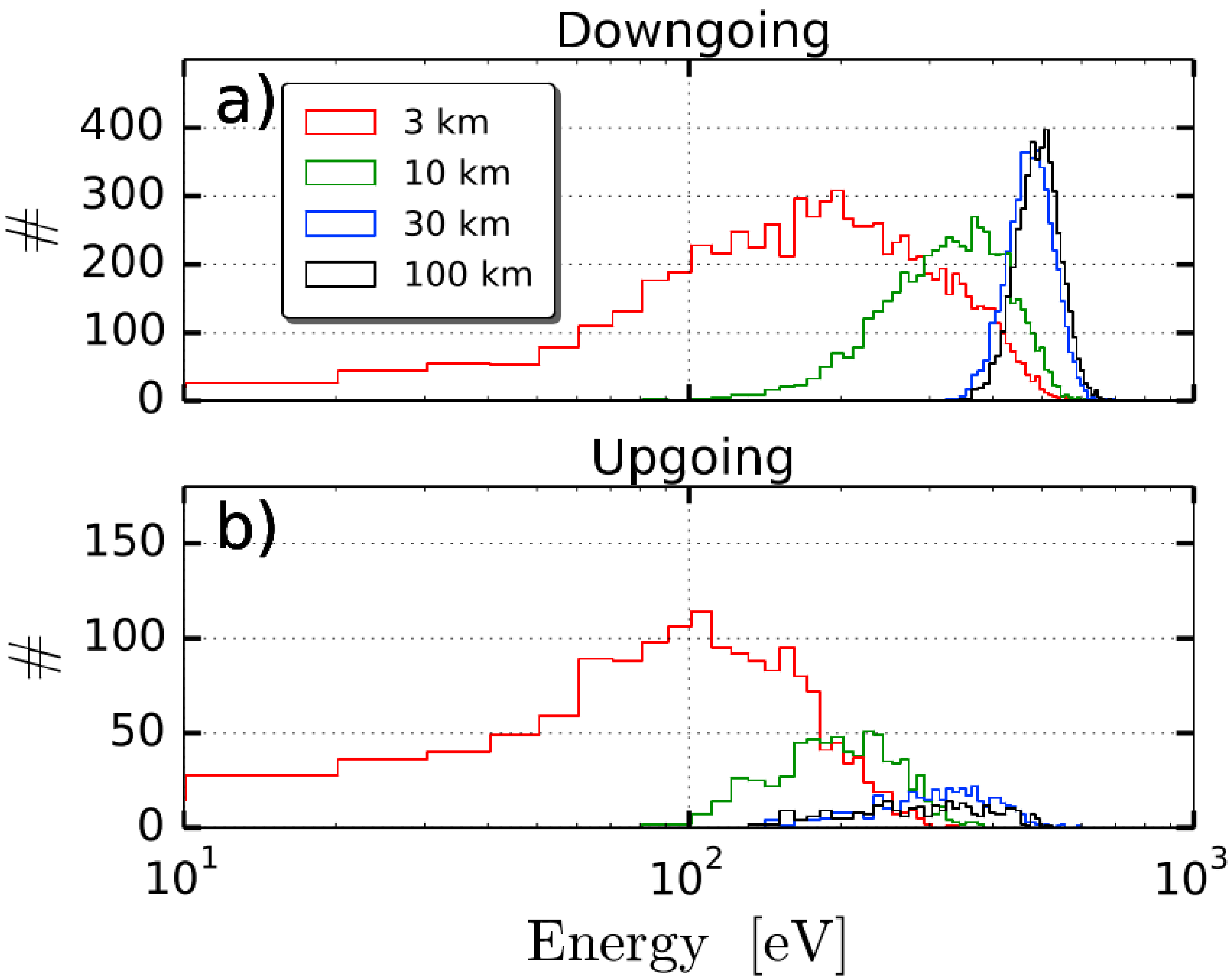

Downgoing
a)
3 km
10 km
30 km
100 km
400
300
200
100
0
#
Upgoing
b)
150
100
50
0
#
10^1
10^2
10^3
Energy [eV]

Backup

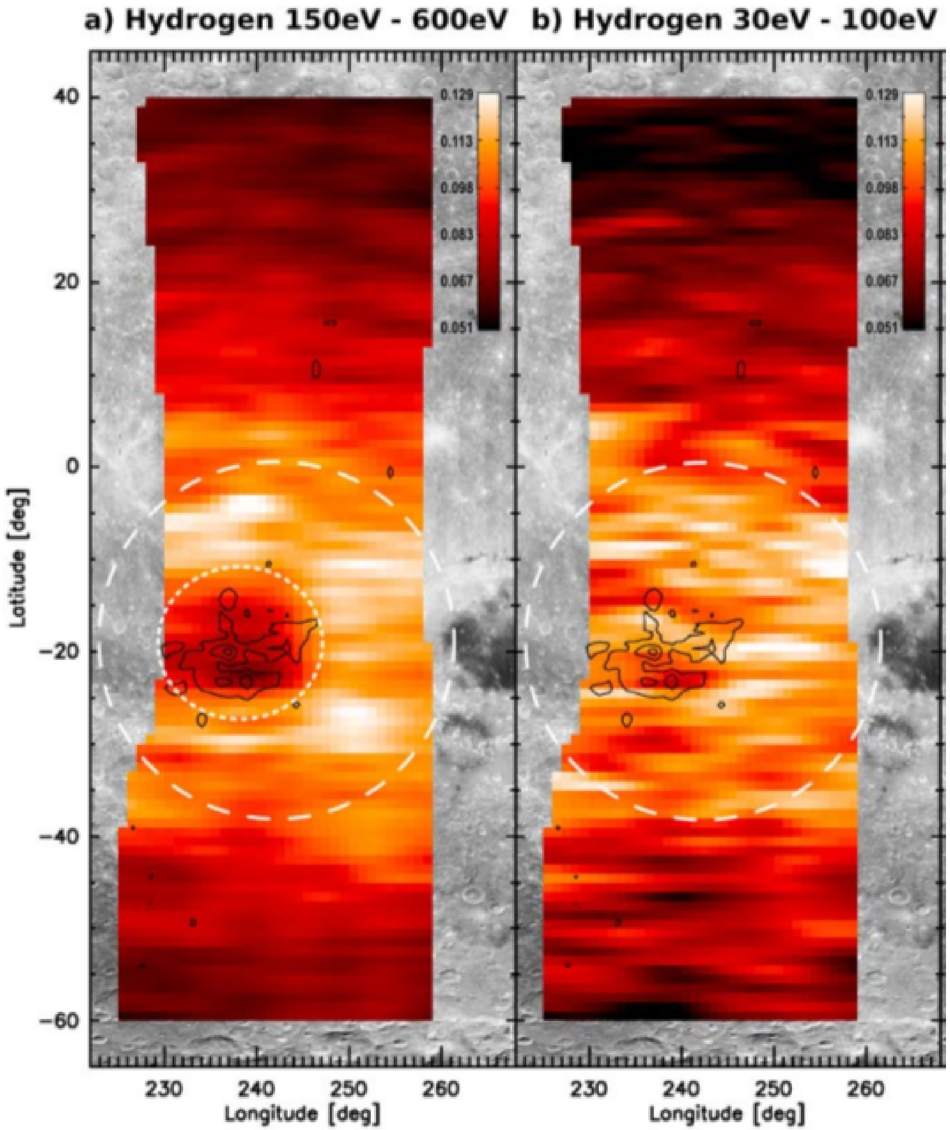

[Wieser et al., 2010]

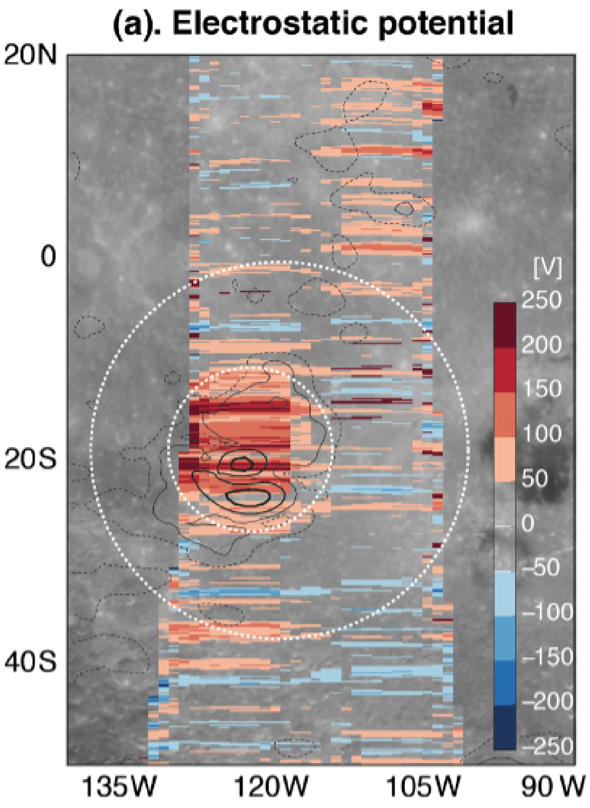

[Futaana et al., 2013]

Backup

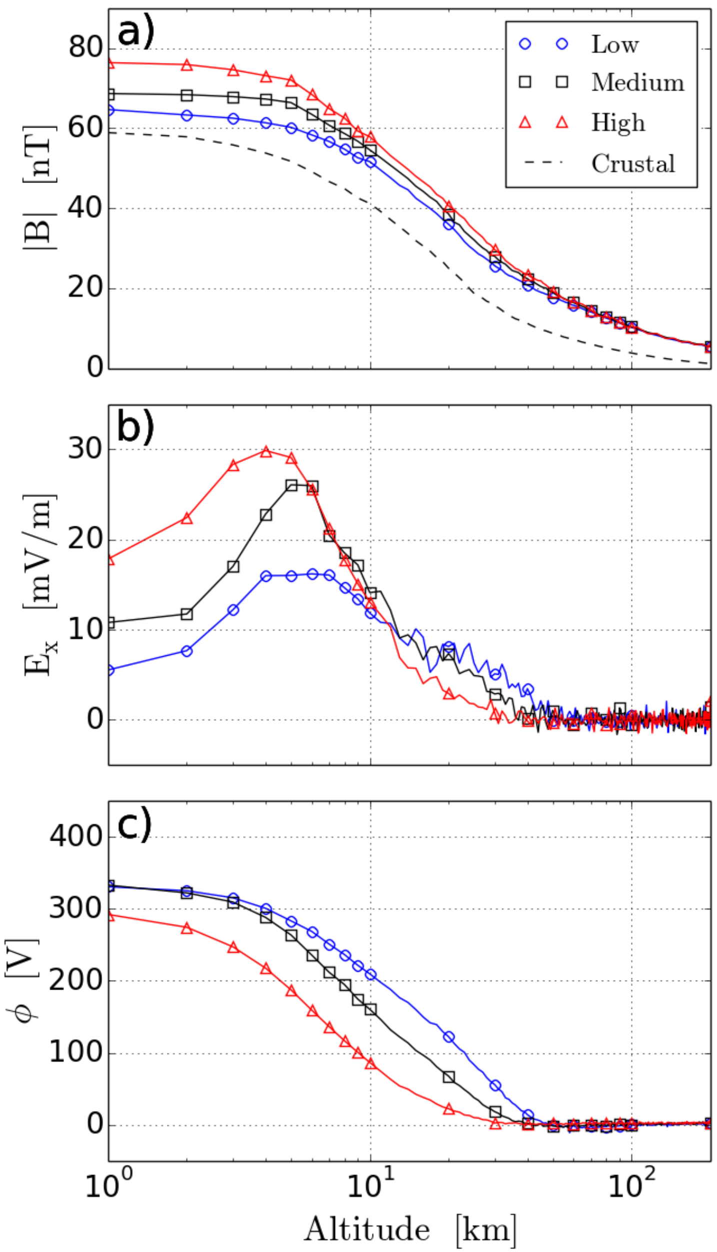

a)
b)
c)
Low
Medium
High
Crustal
|B| [nT]
E_x [mV/m]
ϕ [V]
Altitude [km]
0
20
40
60
80
0
10
20
30
0
100
200
300
400
10^0
10^1
10^2

Medium

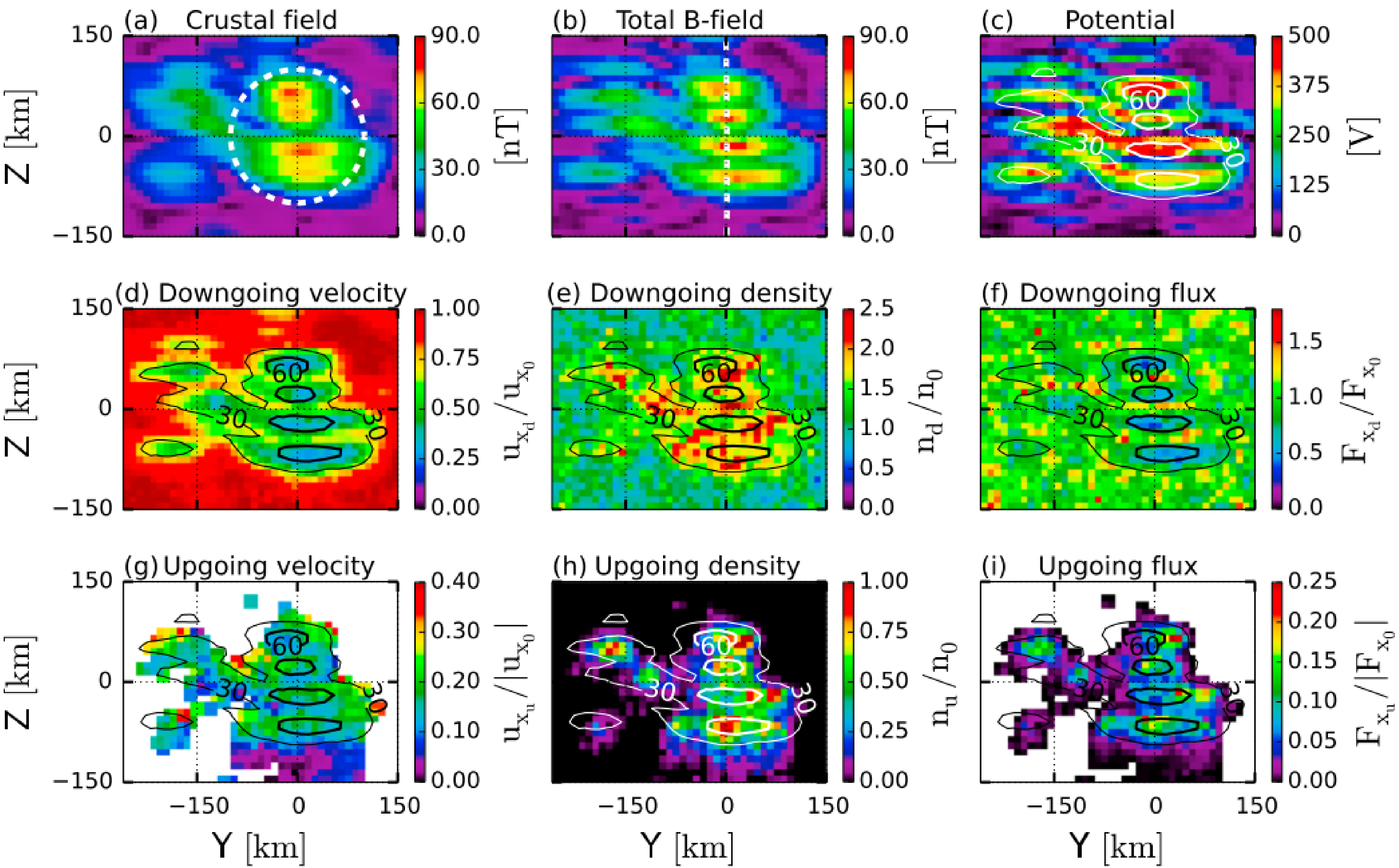

(a) Crustal field
(b) Total B-field
(c) Potential
(d) Downgoing velocity
(e) Downgoing density
(f) Downgoing flux
(g) Upgoing velocity
(h) Upgoing density
(i) Upgoing flux
Z [km]
Y [km]
150
0
−150
−150
0
150
90.0
60.0
30.0
0.0
[nT]
500
375
250
125
0
[V]
1.00
0.75
0.50
0.25
0.00
u_{x_d}/u_{x_0}
2.5
2.0
1.5
1.0
0.5
0.0
n_d/n_0
1.5
1.0
0.5
0.0
F_{x_d}/F_{x_0}
0.40
0.30
0.20
0.10
0.00
$u_{x_u}/|u_{x_0}|$
n_u/n_0
0.25
0.20
0.15
0.10
0.05
0.00
$F_{x_u}/|F_{x_0}|$
60
30

Low

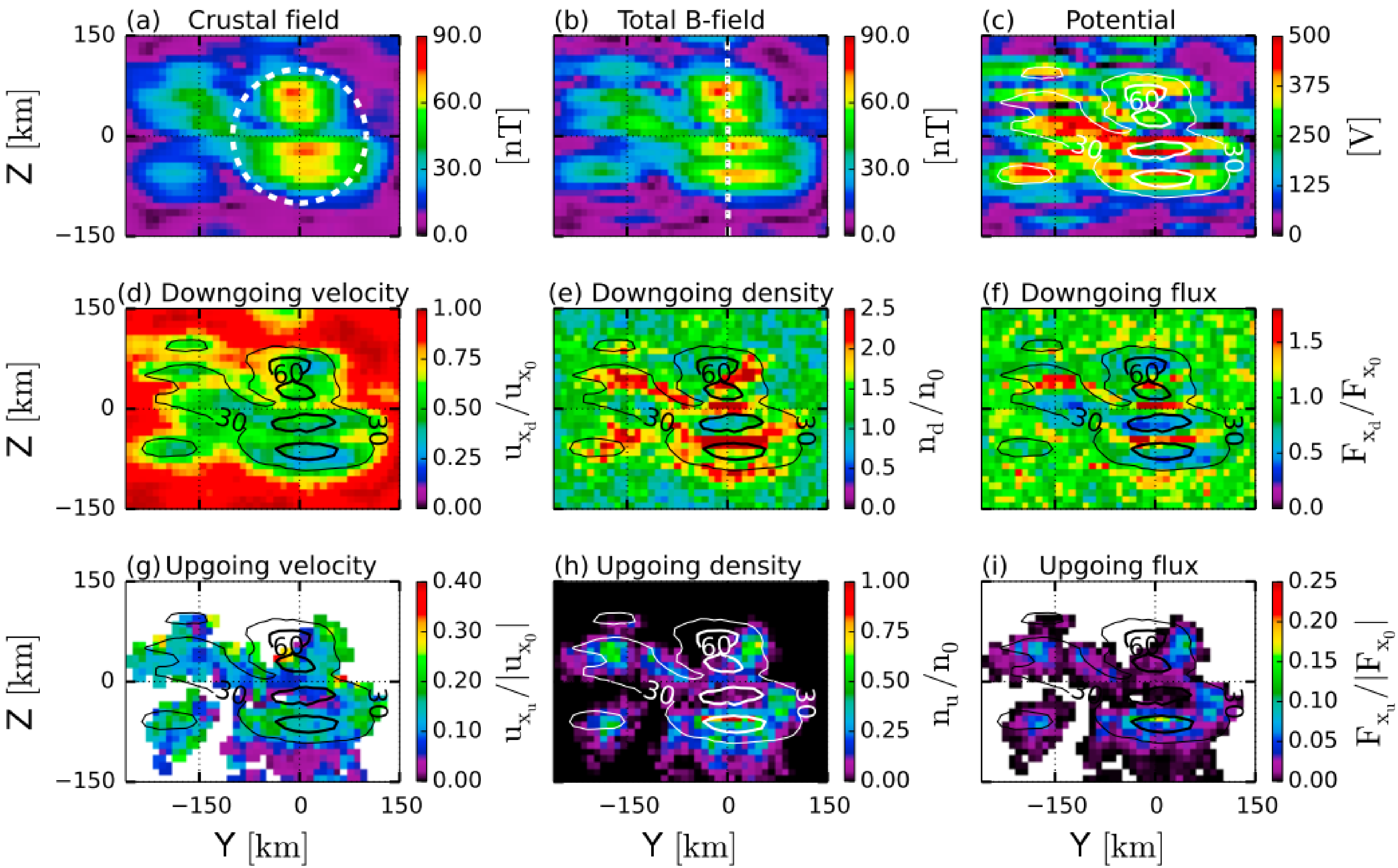

(a) Crustal field
(b) Total B-field
(c) Potential
(d) Downgoing velocity
(e) Downgoing density
(f) Downgoing flux
(g) Upgoing velocity
(h) Upgoing density
(i) Upgoing flux
Z [km]
Y [km]
[nT]
[V]
u_{x_d}/u_{x_0}
n_d/n_0
F_{x_d}/F_{x_0}
$u_{x_u}/|u_{x_0}|$
n_u/n_0
$F_{x_u}/|F_{x_0}|$

High

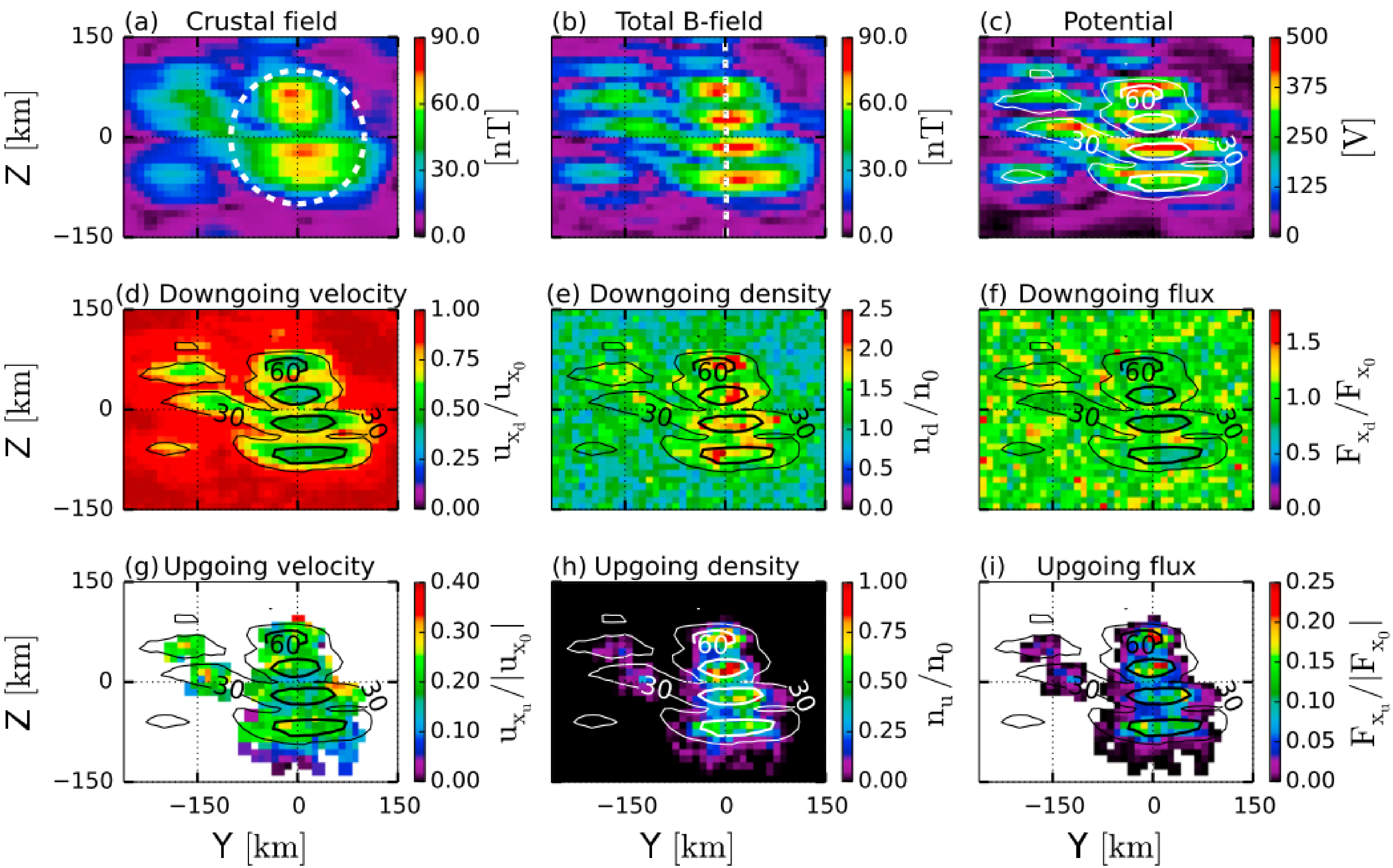

(a) Crustal field
(b) Total B-field
(c) Potential
(d) Downgoing velocity
(e) Downgoing density
(f) Downgoing flux
(g) Upgoing velocity
(h) Upgoing density
(i) Upgoing flux
Z [km]
Y [km]
150
0
−150
−150
0
150
90.0
60.0
30.0
0.0
[nT]
500
375
250
125
0
[V]
1.00
0.75
0.50
0.25
0.00
u_{x_d}/u_{x_0}
2.5
2.0
1.5
1.0
0.5
0.0
n_d/n_0
1.5
1.0
0.5
0.0
F_{x_d}/F_{x_0}
0.40
0.30
0.20
0.10
0.00
$u_{x_u}/|u_{x_0}|$
1.00
0.75
0.50
0.25
0.00
n_u/n_0
0.25
0.20
0.15
0.10
0.05
0.00
$F_{x_u}/|F_{x_0}|$
60
30